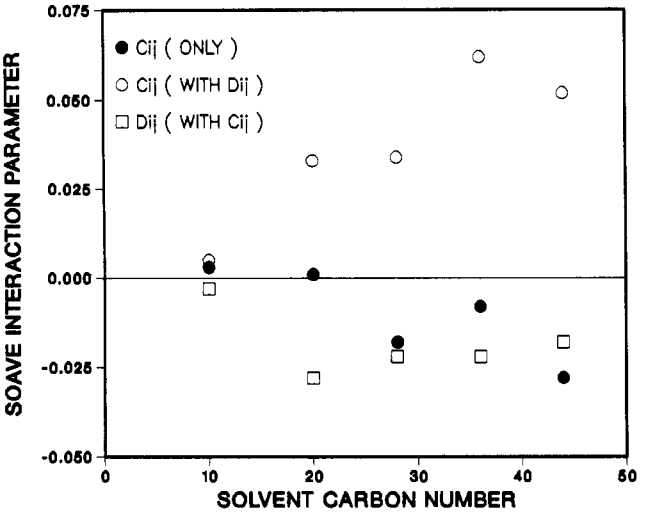

Figure 5. Soave interaction parameters, C_{ij} and D_{ij}, for ethane + heavy *n*-paraffins.

z mole fraction (liquid or vapor phase)

Registry No. *n*-C_{20}, 112-95-8; *n*-C_{28}, 630-02-4; *n*-C_{36}, 630-06-8; *n*-C_{44}, 7098-22-8; C_2H_6, 74-84-0.

Literature Cited

(1) Gasem, K. A. M.; Robinson, Jr., R. L. *J. Chem. Eng. Data* **1985**, *30*, 53-56.
(2) Anderson, J. M.; Barrick, M. W.; Robinson, Jr., R. L. *J. Chem. Eng. Data* **1986**, *31*, 172-175.
(3) Gupta, M. K.; Li, Y.-H.; Hulsey, B. J.; Robinson, Jr., R. L. *J. Chem. Eng. Data* **1982**, *27*, 55-57.
(4) Anderson, J. M.; Barrick, M. W.; Robinson, Jr., R. L. *J. Chem. Eng. Data* **1987**, *32*, 372-374.
(5) Gasem, K. A. M.; Robinson, Jr., R. L. Paper presented at the Spring National Meeting of the American Institute of Chemical Engineers, Houston, TX, March 24-28, 1985.
(6) Bufkin, B. A.; Robinson, Jr., R. L.; Estera, S. S.; Luks, K. D. *J. Chem. Eng. Data* **1986**, *31*, 421-423.
(7) Anderson, J. M. M.S. Thesis, Oklahoma State University, Stillwater, OK, May 1985.
(8) Barrick, M. W. M.S. Thesis, Oklahoma State University, Stillwater, OK, May 1985.
(9) Ross, C. H. M.S. Report, Oklahoma State University, Stillwater, OK, December 1987.
(10) Goodwin, R. D.; Roder, H. M.; Straty, G. C. *NBS Tech. Note* **1976**, *No. 684*.
(11) Doolittle, A. K.; Peterson, R. H. *J. Am. Chem. Soc.* **1951**, *73*, 2145.
(12) Peters, C. J.; Roo, J. L.; Lichtenthaler, R. N. *Fluid Phase Equilib.* **1987**, *34*, 287-308.
(13) Huang, S. H.; Lin, H. M.; Chao, K. C. *J. Chem. Eng. Data* **1986**, *33*, 145-147.
(14) Luks, K. Personal Communication, University of Tulsa, 1988.
(15) Huang, S. H.; Lin, H. M.; Chao, K. C. *J. Chem. Eng. Data* **1988**, *33*, 143-145.
(16) Chao, K. C.; Lin, H. M. *Synthesis Gas Solubility in Fischer-Tropsch Slurry*; DE-AC22-84PC70024, final report, Department of Energy; Government Printing Office: Washington, DC, July 1987.
(17) Soave, G. *Chem. Eng. Sci.* **1972**, *15*, 1197-1203.
(18) Peng, D.-Y.; Robinson, D. B. *Ind. Eng. Chem. Fundam.* **1976**, *15*, 59-64.
(19) Ely, J. F.; Hanley, J. M. *NBS Tech. Note* **1981**, *No. 1039*.

Received for review May 10, 1986. Accepted November 14, 1988. This work was supported by the U.S. Department of Energy under Contract No. DE-FG22-86-PC90523.

Equilibrium Phase Compositions, Phase Densities, and Interfacial Tensions for CO_2 + Hydrocarbon Systems. 5. CO_2 + *n*-Tetradecane

K. A. M. Gasem, K. B. Dickson,† P. B. Dulcamara,‡ N. Nagarajan,§ and R. L. Robinson, Jr.*

School of Chemical Engineering, Oklahoma State University, Stillwater, Oklahoma 74078

Experimental vapor-liquid phase compositions, phase densities, and interfacial tensions are presented for CO_2 + *n*-tetradecane at 160 °F and pressures from 1000 psia to the critical point (interfacial tensions as low as 0.01 mN/m). These data, in combination with our previously reported results for CO_2 + *n*-butane and CO_2 + *n*-decane, provide useful information on the effects of molecular size on the behavior of CO_2 + *n*-paraffin systems.

Introduction

The work presented here is part of our continuing studies on phase behavior and interfacial tension (IFT) in mixtures of CO_2 (and ethane) with a series of hydrocarbon solvents, including pure and mixed hydrocarbons and reservoir oils. The present data on CO_2 + *n*-tetradecane complement our previous results for CO_2 + *n*-butane (*1*) and CO_2 + *n*-decane (*2*). The combined results now provide information on the behavior of CO_2 in 4-, 10- and 14-carbon *n*-paraffin solvents. These data provide a basis for developing/testing models for representation of such data and, more particularly, permit evaluation of model parameters (e.g., binary interaction parameters) which may be generalized to permit interpolation or extrapolation for describing the behavior of systems involving *n*-paraffins of different molecular sizes.

Experimental Method

The experimental facility and procedures have been described in detail previously (*1-3*). Several modifications have been made for the present work, as described below.

Initial measurements on the present mixtures produced vapor densities that appeared to be too high. After considerable investigation of the causes for this, a second Mettler/Parr vibrating U-tube densitometer was installed. The densitometer used for vapor-phase measurements was positioned slightly above the vapor-liquid interface in the windowed equilibrium cell, and the liquid densitometer was positioned below the interface. Each was mounted in a vertical position; the vapor densitometer was installed with the bend in the U-tube at the

† Present address: Exxon Production Research Co., P.O. Box 2169, Houston, TX 77252-2189.
‡ Present address: DOW Chemical U.S.A., Texas Operations, Freeport, TX 77541.
§ Present address: Mobil Research and Development Corp., P.O. Box 819047, Dallas, TX 75381-9047.

0021-9568/89/1734-0191$01.50/0

Table I. Phase Equilibria and Interfacial Tensions for Carbon Dioxide + *n*-Tetradecane at 344.3 K (160 °F)

phase composns, mole fraction of CO_2				phase densities × 10^{-3}, kg/m^3				IFT-density diff ratio	
liquid phase		vapor phase		liquid phase		vapor phase			
press., psia	x	press., psia	y	press., psia	ρ^L	press., psia	ρ^V	press., psia	$\gamma/\Delta\rho \times 10^3$, (mN/m)/(kg/m^3)
		1027	0.989			1029	0.1466		
		1204	0.989			1204	0.1827		
		1307	0.988			1306	0.2076		
		1506	0.991			1504	0.2640		
1606	0.685	1603	0.992	1601	0.7508	1602	0.2966	1602	8.95
1694	0.711	1696	0.991	1694	0.7514	1695	0.3324	1693	7.85
1787	0.738	1788	0.992	1787	0.7525	1787	0.3708	1787	6.48
1902	0.769	1900	0.988	1900	0.7545	1899	0.4251	1901	5.48
2025	0.797	2017	0.987	2025	0.7551	2017	0.4861	2022	4.00
2025	0.797	2017	0.987	2025	0.7551	2017	0.4861	2022	4.26
2111	0.819	2102	0.984	2101	0.7546	2101	0.5303	2106	3.22
2153	0.827	2145	0.983	2153	0.7541	2144	0.5532	2148	2.93
2194	0.839	2197	0.983	2190	0.7528	2190	0.5766	2188	2.32
2256	0.857	2256	0.976	2255	0.7523	2256	0.6102	2256	1.43
2276	0.862	2274	0.976	2275	0.7504	2273	0.6165	2272	1.22
2309	0.870	2296	0.971	2307	0.7486	2307	0.6321	2307	0.790
2325	0.877	2315	0.968	2324	0.7458	2324	0.6411	2324	0.700
2341	0.885	2340	0.965	2342	0.7442	2342	0.6544	2342	0.445
2353	0.887	2346	0.964	2354	0.7409	2354	0.6598	2354	0.296
2363	0.893	2360	0.960	2360	0.7388	2360	0.6659	2361	0.195
2364	0.895	2364	0.958	2361	0.7373	2361	0.6670	2365	0.173
2372	0.899	2365	0.955	2365	0.7365	2365	0.6705		

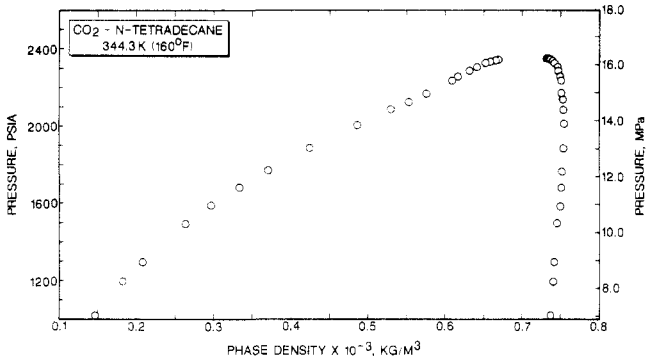

Figure 1. Phase densities for CO_2 + *n*-tetradecane at 160 °F.

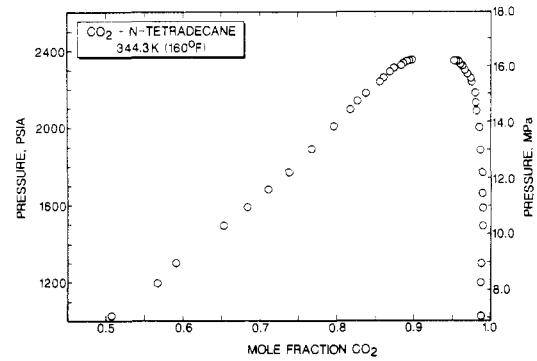

Figure 2. Phase compositions for CO_2 + *n*-tetradecane at 160 °F.

top so liquid would drain from the tube, and the liquid densitometer was positioned with the U-bend at the bottom to facilitate displacement of vapor bubbles from the tube. Subsequent measurements yielded improved vapor densities; this is believed to result primarily from improved drainage of liquid from the vapor densitometer.

In the pendant-drop IFT cell, the two smallest diameter needles were replaced by larger needles into which small wires were inserted. These small diameter wires protrude from the ends of the needles, and drops were formed on the wires rather than needle tips. These drops were smaller than those obtained on the available needles.

The phase compositions were measured by gas chromatography using columns containing 3.7 ft of Porapak Q and 5.7 ft of OV-101 in series. A thermal conductivity dector was employed in all analyses; the response factor was determined to be 0.26, based on analyses of volumetrically prepared mixtures of known composition.

Materials

The CO_2 was supplied by Union Carbide Linde Division and had a stated purity of 99.99%. The *n*-tetradecane was from Alfa Products with a purity of 99%. The chemicals were used without further purification.

Experimental Results

The measured data appear in Table I and are illustrated in Figures 1–3. Table I contains values of $\gamma/\Delta\rho$ since these are

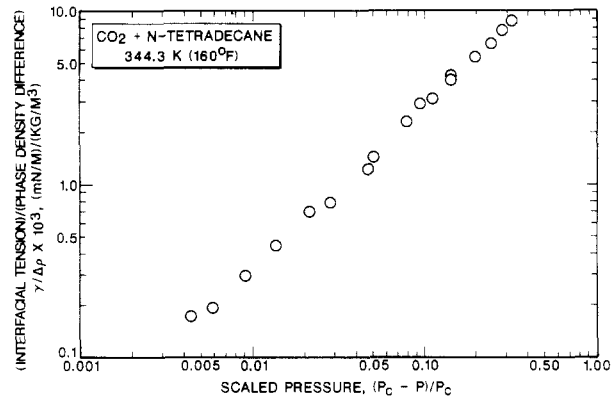

Figure 3. Interfacial tension–phase density difference ratios for CO_2 + *n*-tetradecane at 160 °F.

the quantities determined from photographs of the pendant drops in the IFT cell. No liquid densities, liquid compositions, or $\gamma/\Delta\rho$ values are reported at pressures below 1600 psia because adequate liquid circulation was not obtained, while vapor circulation was satisfactory. In Figure 3, the $\gamma/\Delta\rho$ values are plotted as a function of "scaled" pressure because (a) this conveniently expands the near-critical, low-IFT region and (b) "scaling laws" require that this relationship becomes linear (log–log) as the critical pressure is approached and that the slope should be a specific, universal value, independent of the substances studied. Smoothed (interpolated and extrapolated) properties are given in Table II; the methods employed

Table II. Smoothed Phase Equilibria and Interfacial Tensions for Carbon Dioxide + *n*-Tetradecane at 344.3 K (160 °F)

press.		phase composns, mole fraction of CO_2		phase densities $\times 10^{-3}$, kg/m^3		interfacial tension,
kPa	psia	liquid	vapor	liquid	vapor	mN/m
6895	1000		0.989		0.1417	
7585	1100		0.988		0.1600	
8275	1200		0.988		0.1818	
8963	1300		0.989		0.2061	
9650	1400		0.990		0.2328	
10340	1500		0.991		0.2626	
11030	1600	0.683	0.991	0.7508	0.2961	4.03
11270	1700	0.713	0.991	0.7415	0.3342	3.23
12410	1800	0.742	0.990	0.7529	0.3772	2.49
13100	1900	0.768	0.989	0.7542	0.4252	1.81
13790	2000	0.792	0.987	0.7550	0.4769	1.22
14480	2100	0.815	0.985	0.7548	0.5303	0.728
15170	2200	0.840	0.981	0.7531	0.5818	0.360
15860	2300	0.869	0.972	0.7489	0.6294	0.113
15925	2310	0.873	0.970	0.7481	0.6342	0.094
15995	2320	0.876	0.969	0.7471	0.6392	0.077
16065	2330	0.879	0.967	0.7459	0.6445	0.060
16135	2340	0.883	0.965	0.7443	0.6504	0.044
16200	2350	0.887	0.962	0.7420	0.6572	0.029
16215	2352	0.888	0.962	0.7414	0.6587	0.026
16230	2354	0.888	0.961	0.7408	0.6603	0.024
16245	2356	0.889	0.960	0.7401	0.6620	0.021
16255	2358	0.890	0.960	0.7394	0.6638	0.018
16270	2360	0.891	0.959	0.7385	0.6657	0.016
16285	2362	0.892	0.958	(0.7375)[a]	(0.6678)	(0.013)
16300	2364	0.893	0.957	(0.7364)	(0.6701)	(0.011)
16315	2366	0.894	(0.955)	(0.7351)	(0.6727)	(0.009)
16325	2368	0.896	(0.954)	(0.7336)	(0.6755)	(0.007)
16340	2370	0.898	(0.952)	(0.7316)	(0.6789)	(0.005)
16355	2372	0.900	(0.949)	(0.7291)	(0.6831)	(0.003)
16370	2374	(0.903)	(0.945)	(0.7252)	(0.6889)	(0.001)
16380[b]	2376	(0.924)	(0.924)	(0.7085)	(0.7085)	(0.000)

[a] Numbers in parentheses are extrapolations beyond highest measured pressures. [b] Estimated critical point (visual observation gave 2374 ± 2 psia).

to generate this table are described in Appendix A. Table II contains estimates of the critical-point pressure, composition, and density for CO_2 + *n*-tetradecane at 160 °F. These estimates are the values that produced optimum description of the phase properties using the smoothing functions described in Appendix A. The P_c value (2376 psia) is in excellent agreement with the visual observation in the equilibrium cell (2374 ± 2 psia).

On the basis of our experience with the systems studied to date, we estimate the experimental inaccuracies in the data to be 0.003 in mole fraction, 0.001 g/cm^3 in density, and $0.04\gamma^{0.8}$ for IFT. The smoothed values in Table II retain this level of accuracy.

No previous IFT data are available for comparison with the present measurements. However, Bufkin (*4*) has measured solubilities of CO_2 in *n*-tetradecane using the technique described by Anderson et al. (*5*). In the range of overlap of the two data sets (1675–1900 psia), the results are in good agreement, with Bufkin's solubility values being lower by 0.003–0.006 mole fraction of CO_2 (Table III). Thus, the data of Bufkin can be used to extend the present liquid-phase-composition measurements to lower pressures.

Pollack et al. (*6*) have also reported data on the present system at 343.3 K (158.3 °F). Their (interpolated) critical properties are approximately as follows: P_c = 2395 psia and z_c = 0.945 mole fraction of CO_2. Thus, their critical pressure is 20 psi higher and the critical composition 0.02 higher than the present work. At pressures in the range from 2100 to 2350 psi, their saturated-phase compositions are on the order of 0.005 mole fraction of CO_2 higher than the present work.

Table III. Comparisons of Liquid-Phase-Composition Measurements

	liquid mole fraction of CO_2	
press., psia	ref *4*	this work (smoothed)
224.5	0.136	
460.0	0.260	
800.0	0.410	
1065.0	0.509	
1677.0	0.703	0.706
1748.5	0.721	0.727
1892.0	0.762	0.766

As a result of our initial difficulties with measurements of vapor-phase densities, we sought confirmation of our results. In response to our request, both Creek (*7*) and Metcalfe and Raby (*8*) made selected density measurements on this system. In addition, we performed vapor density measurements using a different experimental method. Details appear in Appendix B, and the results of the combined measurements reinforce our estimate of the accuracy of the present results.

Conclusion

Data are presented for phase compositions, phase densities, and IFTs at 160 °F for CO_2 + *n*-tetradecane. The accuracy of these results appears comparable to our previously reported data (*1–3*). The present data contain information not previously available in the literature.

Appendix A

Experimental measurements on the present apparatus are performed much more easily and efficiently if the individual properties (x, y, ρ^L, ρ^V, and $\gamma/\Delta\rho$) are each obtained at a slightly different pressure (e.g., ±5 psi from the "nominal" pressure of interest). Such a procedure eliminates the tedious adjustment of pressure prior to each individual measurement. Although this is convenient from an experimental standpoint, the resultant data are not in an optimum form for users of the data. Thus, formulas have been employed for interpolation and extrapolation of the measured values so that the results can be presented in a more directly usable form. Such formulas, to be of value, should (a) represent the data within their experimental uncertainties and (b) obey known power law behavior as the critical point is approached. The functions described below have been found to fulfill these requirements.

Wichterle et al. (*9*) and Charoensombut-amon et al. (*10*) employed functions of the type shown below to represent the difference between an "order parameter, ϕ", in two equilibrium phases (denoted by + and −):

$$\phi_+ - \phi_- = \sum_{i=0}^{N} B_i (P^*)^{\beta+i\Delta} \qquad \text{(A1)}$$

where the leading term (i = 0) is the limiting "power (scaling) law" behavior of the order parameter, ϕ, and the subsequent terms in the summation are Wegner (*11*) corrections to the scaling behavior.

If the above relation is coupled with an equation for the "rectilinear diameter" of the form

$$(\phi_+ + \phi_-)/2 = \phi_c + A_0(P^*)^{1-\alpha} + \sum_{j=1}^{M} A_j (P^*)^j \qquad \text{(A2)}$$

then these expressions may be combined to yield ϕ_+ and ϕ_- individually as

$$\phi_\pm = \phi_c + A_0(P^*)^{1-\alpha} + \sum_{j=1}^{M} A_j (P^*)^j \pm \frac{1}{2}\sum_{i=0}^{N} B_i (P^*)^{\beta+i\Delta} \qquad \text{(A3)}$$

where $\phi_+ \equiv \phi^L$ and $\phi_- \equiv \phi^V$. The real value of the above formalism is that the exponents α, β, and Δ are universal

Table IV. Parameters Used To Generate Smoothed Properties in Table II

param	estimate	param	estimate
	Phase Compositions[a] (Eq A3)[a]		
z_c	0.923 793 86	B_0	0.525 092 89
A_0	0.981 137 28	B_1	-3.397 188 92
A_1	-1.680 212 54	B_2	21.023 701 93
A_2	2.323 441 37	B_3	-60.241 331 69
A_3	-6.545 411 47	B_4	83.203 390 46
A_4	6.413 709 32	B_5	-43.197 726 93
A_5	0.233 753 71		
	Phase Densities[b] (Eq A3)		
ρ_c	0.708 492 23	B_0	0.370 802 81
A_0	-1.407 925 17	B_1	0.695 666 41
A_1	1.719 197 72	B_2	-9.380 003 50
A_2	-5.511 694 09	B_3	42.696 974 60
A_3	17.244 838 88	B_4	-67.995 715 66
A_4	-25.378 074 71	B_5	36.728 913 74
A_5	15.666 131 72		
	IFT-Density Difference Ratio[c] (Eq A4)		
G_0	22.063 492 13	G_f	5.162 560 39

[a] Units: mole fraction of CO_2. [b] Units: $(kg/m^3) \times 10^{-3}$ or g/cm^3. [c] Units: $[(mN/m)/(kg/m^3)] \times 10^3$ or $[(mN/m)/(g/cm^3)]$.

constants, independent of the fluid of interest. An approach similar to the above has been discussed by Nagarajan (*12*).

Charoensombut-amon used eq A3 to fit isothermal $P-x,y$ data ($\phi_+ = y$, $\phi_- = x$) for CO_2 + *n*-hexadecane using $\beta = {}^1/_3$, $\alpha = {}^1/_8$, $\Delta = {}^1/_2$, $M = 3$, and $N = 6$, for a total of 12 constants (z_c included).

In the present work, eq A3 has been used to represent the P vs ρ^L, ρ^V and P vs x,y behavior with

for $P-\rho^L,\rho^V$:

$$\phi_c = \rho_c, \quad \phi_+ = \rho^L, \quad \phi_- = \rho^V, \quad M = 5, \quad N = 5$$

for $P-x,y$:

$$\phi_c = z_c, \quad \phi_+ = y, \quad \phi_- = x, \quad M = 5, \quad N = 5$$

The values of $\gamma/\Delta\rho$ are expressed as

$$\gamma/\Delta\rho = \sum_{k=0}^{L} G_k (P^*)^{2\nu-\beta+k\Delta} \tag{A4}$$

with $L = 1$.

In the regressions employed to fit the above expressions to the experimental data, values of M, N, and L were set at the minimum values required to represent the data within their estimated experimental precision. In addition, values for P_c and the critical exponents were varied. The calculations were insensitive to the exponents over their accepted ranges (e.g., 0.325 (*13*) to 0.355 (*14*) for β), so the simple values of $\beta = {}^1/_3$ and $\alpha = {}^1/_8$ by Charoensombut-arom were used, as was the generally accepted value of $\nu = 0.63$. Calculations were more sensitive to P_c. The optimum (integer) value of P_c to fit all data (x, y, ρ^V, ρ^L, $\gamma/\Delta\rho$) simultaneously was found to be 2376 psia, in good agreement with the visually determined experimental pressure of 2374 ± 2 psia.

The parameters used to smooth the data appear in Table IV. These results are based on weighted regressions of the data; i.e., the sum of squares of weighted residuals (SS) was minimized:

$$SS = \sum_{i=1}^{K} [(Y^{calcd} - Y^{exptl})/\sigma_Y]_i^2 = \sum_{i=1}^{K} (\Delta Y/\sigma_Y)_i^2$$

where K is the number of experimental observations and

$$\sigma_Y^2 \equiv \epsilon_Y^2 + (\partial Y/\partial P)^2 \epsilon_P^2$$

Y denotes the compositions (x, y), densities (ρ^L, ρ^V), or IFT-to-density difference ratio ($\gamma/\Delta\rho$). The experimental uncertainties, ϵ, were taken to be the following in the regressions:

$$\epsilon_x = \epsilon_y = 0.0007$$

$$\epsilon_\rho{}^V = \epsilon_\rho{}^L = 0.0002 \text{ g/cm}^3$$

$$\epsilon_{\gamma/\Delta\rho} = 0.037(\gamma/\Delta\rho)^{0.8}$$

$$\epsilon_P = 0.5 \text{ psia}$$

The values are measures of precision, rather than accuracy, of the measurements; as discussed previously, estimated inaccuracies are generally larger than these values.

The final values for the parameters used to describe the data are given in Table IV and were determined as follows. First, regressions were performed with all measured data points included and the results were analyzed. Next, any data point having a weighted deviation, $\Delta Y/\sigma_Y$, larger than 2.5 was discarded, and the final regressions were performed on the reduced data set. This procedure resulted in deletion of only one density value (ρ^V at 2342 psia).

The weighted-root-mean-square deviations for the fit of the equations to the data are 0.96 for x, y, 0.96 for ρ^V, ρ^L, and 1.09 for $\gamma/\Delta\rho$. The corresponding root-mean-square residuals are 0.0010 for mole fractions, 0.00041 g/cm^3 for densities, and 0.108 (mN/m)/(g/cm^3) or 3.6% for $\gamma/\Delta\rho$. Although the residuals retain some systematic behavior, they are within the experimental uncertainties in the data.

The extrapolated property values (beyond the highest measured pressures) shown in parentheses in Table II are believed to be reliable since they are in the near-critical power-law region, which is described correctly by the formulas. However, these formulas are not suitable for extrapolations to pressures lower than those given in Table II.

Appendix B

At our request, density measurements were performed by Creek (*7*) and Metcalfe and Raby (*8*), specifically to assess the accuracy of the density measurements of the present work. Metcalfe and Raby used a high-pressure pycnometer, and Creek employed volumetric displacement of vapor from a high-pressure equilibrium cell to a low-pressure collection vessel for gravimetric analysis. In addition, we made density determinations by a material balance method, which employs the following relations:

$$m = m^L + m^V \tag{B1}$$

or

$$m = \rho^L f^L V + \rho^V (1 - f^L) V \tag{B2}$$

and

$$\rho^V = \frac{(m/V) - f^L \rho^L}{1 - f^L} \tag{B3}$$

Thus, ρ^V was calculated by this material balance relation from a series of measurements made of the total system volume (V), the total mass (m) of fluid injected into the cell, the volume fraction liquid (f^L) in the cell, and the liquid density (ρ^L). The liquid densities from our densitometer measurements were accepted as being correct.

A comparison of the various density data appears in Figure 4. The data are concentrated in the region above 2100 psia because in this region errors in ρ^V or ρ^L have large effects on $\Delta\rho$, which in turn affects the γ calculated from the pendant-drop $\gamma/\Delta\rho$ measurements. Uncertainty estimates of 0.005 g/cm^3 for Metcalfe/Raby and 0.001 for Creek were provided by these investigators. For liquid densities, the various data typically scatter by less than 0.5% (i.e., ~0.004 g/cm^3) from the mean value. The present data agree very well with Creek's results at 2285 psia and above, and they are in exact agree-

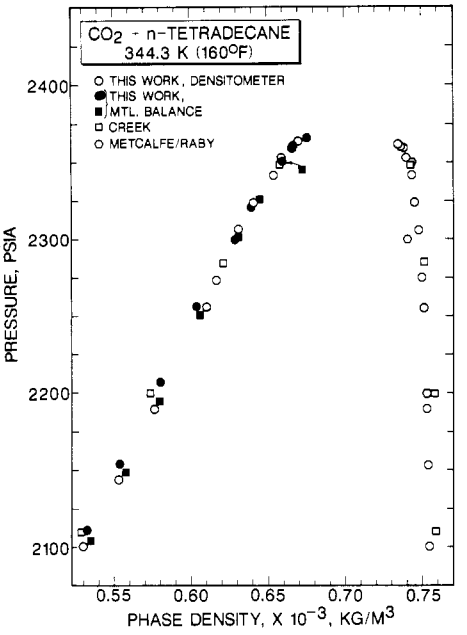

Figure 4. Comparison of phase density measurements.

ment with Metcalfe and Raby at 2200 psia.

For vapor densities, the present results agree very well with Creek's data at 2285 psia and above (differences less than 0.002 g/cm^3), with larger differences at lower pressures. The estimated uncertainty in our material balance densities is 0.005 g/cm^3 (~0.8%). Two separate runs were made, which generally deviate in opposite directions from our densitometer results. The average of the two material balance runs differs by no more than 0.002 g/cm^3 from the densitometer results.

Probably the major conclusion to be drawn from the above analyses is that various investigators are likely to produce saturated-phase densities that are consistent to no better than about 1%.

Glossary

A_i, B_i, G_i	parameters in eq A1-A4
f^L	volume fraction liquid in equilibrium cell
m	total mass in equilibrium cell
m^L	mass of liquid in equilibrium cell
m^V	mass of vapor in equilibrium cell
P	pressure
P_c	critical pressure
P^*	scaled pressure, $(P_c - P)/P_c$
V	total volume of equilibrium cell
x	liquid-phase mole fraction
y	vapor-phase mole fraction
Y	general experimental variable
z_c	critical composition (mole fraction)

Greek Letters

α, β, ν	scaling-law parameters (critical indices)
γ	interfacial tension
ϵ_Y	uncertainty in measured variable Y
ρ^L	liquid-phase density
ρ^V	vapor-phase density
ρ_c	critical density
$\Delta\rho$	liquid-phase density minus vapor-phase density
ϕ	general "order parameter"

Registry No. CO_2, 124-38-9; tetradecane, 629-59-4.

Literature Cited

(1) Hsu, Jack J. C.; Nagarajan, N.; Robinson, Jr., R. L. *J. Chem. Eng. Data* **1985**, *30*, 485.
(2) Nagarajan, N.; Robinson, Jr., R. L. *J. Chem. Eng. Data* **1986**, *31*, 168.
(3) Nagarajan, N.; Robinson, Jr., R. L. *J. Chem. Eng. Data* **1987**, *32*, 369.
(4) Bufkin, B. L. Personal communication, Oklahoma State University, Stillwater, OK, 1985.
(5) Anderson, J. M.; Barrick, M. W.; Robinson, Jr., R. L. *J. Chem. Eng. Data* **1986**, *31*, 172.
(6) Pollack, N. R.; Enick, R. M.; Mangone, D. J.; Morsi, B. I. *SPE Reservoir Eng.* **1988**, *May*, 533.
(7) Creek, J. L., Personal communication, Chevron Oil Field Research Co., La Habra, CA, 1985.
(8) Metcalfe, R. S.; Raby, J. Personal communication, Amoco Production Co., Tulsa, OK, 1984.
(9) Wichterle, I.; Chappelear, P. S.; Kobayashi, R. J. *Comput. Phys.* **1971**, *7*, 606.
(10) Charoensombut-amon, T.; Martin, R. J.; Kobayashi, R. *Fluid Phase Equilib.* **1986**, *31*, 89.
(11) Wegner, F. J. *Phys. Rev.* **1972**, *85*, 4529.
(12) Nagarajan, N.; Kumar, A.; Gopal, E. S. R.; Greer, S. C. *J. Phys. Chem.* **1980**, *84*, 2883.
(13) LeGuillore, J. C.; Zinn-Justin, J. *Phys. Rev. B* **1980**, *21*, 3976.
(14) Levelt-Sengers, J. M. H.; Greer, W. L.; Sengers, J. V. *J. Phys. Chem. Ref. Data* **1976**, *5*, 1.

Received for review August 8, 1988. Accepted October 26, 1988. Financial support for this work was furnished by the following organizations: Amoco Production Research Co., ARCO Oil and Gas Co., Chevron Oil Field Research Co., Marathon Oil Co., Mobil Research and Development Corp., Shell Development Co., Sohio Petroleum Co., Sun Exploration and Production Co., and Texaco, Inc.

Vapor–Liquid Equilibria in Binary Systems Containing Ethanol with Hexamethyldisiloxane and Dimethyl Sulfoxide

Barbara Kaczmarek* and Aleksander Radecki

Department of Physical Chemistry, Medical Academy, 80-416 Gdańsk, Poland

Results of the experimental determination of isobaric vapor–liquid equilibrium data for the binary systems hexamethyldisiloxane (HMDS) with ethanol and ethanol with dimethyl sulfoxide (DMSO) are reported. This work is a continuation of studies on phase equilibria in binary systems (*1–6*).

Reagents

Hexamethyldisiloxane (HMDS) was supplied by CIECH, Gliwice. After purification it had bp 100.8–101 °C, d^{20}_4 = 0.7634 g cm^{-3}, and n^{20}_D = 1.3777.

Dimethyl sulfoxide had bp 189.0 °C, d^{20}_4 = 1.008 g cm^{-3}, and n^{20}_D = 1.4779. Ethanol boiled at 78.3 °C and had d^{20}_4 =

0021-9568/89/1734-0195$01.50/0